Lidar Measurements of the Vertical Absolute Humidity Distribution in the Boundary Layer

CH. WERNER AND H. HERRMANN

Institute of Optoelectronics, German Aerospace Research Establishment (DFVLR), D-8031 Wessling, Federal Republic of Germany

9 December 1979 and 13 January 1981

ABSTRACT

A description is given of a ruby lidar, differential absorption system developed for the measurement of absolute humidity profiles in the atmospheric boundary layer. Two independent temperature controlled ruby lasers are used as transmitters and the backscattered signal from each is digitized and stored separately. Prior to use, the system was calibrated over a horizontal path. Profiles of the absolute humidity have been obtained with a vertical range resolution of 100 m and these are discussed in comparison with radiosonde and airborne measurements.

1. Introduction

One of the parameters that an active meteorological, optical remote sensing station should measure is atmospheric humidity (Blackadar and Droessler, 1977). Some lidar systems suitable for the measurement of atmospheric humidity have been discussed previously[1] (Hinkley, 1976). Raman scattering techniques have been used to determine the water vapor mixing ratio (Inaba and Kobayasi, 1972; Melfi, 1972; Cooney, 1970). Pourny *et al.* (1979) have made similar measurements at night. In the work described here, the goal was the development of a remote sensing technique capable of being operated at any time by technicians. A choice was made of the differential absorption method for this purpose, using two independent ruby lasers. The system has been used in different meteorological conditions over a period of 11 months with measurements made up to an altitude of 1500 m. The operation was both day and night.

2. Principle of measurements

The background of this work was done by Schotland[1] in the early 60's. The method was demonstrated theoretical and experimental (Schotland, 1974; Dobbins and La Grone, 1969). The so-called DASE (differential absorption of scattered energy) or DIAL (differentiation absorption lidar) method is used. Some groups in USSR and China use the same method.[2,3] For a monostatic lidar system pointing to the zenith, the backscattered light is given by the lidar equation

$$P_r(R) = \eta \frac{cJ_tA}{2R^2} \beta \exp\left[-2\int_0^R (\sigma + \rho K_\nu)dr\right], \quad (1)$$

where $P_r(R)$ is the received instantaneous power backscattered from a laser pulse of frequency ν located at a range R, J_t is the transmitted laser energy, η a system constant, c the velocity of light, A the effective aperture of the lidar receiver, β is the atmospheric volume backscattering coefficient, σ the total volume extinction coefficient, $\rho(R)$ is the density of the absorbing gas at range R, and $K_\nu(R)$ is the absorption coefficient of the gas at frequency ν and range R.

Using two transmitted wavelengths for which the absorption cross section differs significantly, i.e., for the on-line and off-line wavelengths or frequencies, one gets the following voltage signal U at the receiver, if the signal noise U_n can be neglected:

[1] R. M. Schotland, 1965: Study of active probing of water vapor profiles and results of experiments. New York University, Geophys. Sci. Lab., Rep. No. 65-6.

[2] V. E. Zuev, B. P. Ivanenko, V. N. Marichev, I. E. Naats, I. V. Samokhvalov and A. V. Sosnin, 1979: Determination of water vapor profiles in the atmosphere using a tunable ruby laser. *Abstracts 9th International Laser Radar Conference*, Munich.

[3] Zhao, Y. S., S. M. Wu, H. S. Jin, C. L. Zhang, and Z. F. Huang, 1979: A DIAL lidar for remote sensing of water vapor profiles. *Abstracts 9th International Laser Radar Conference*, Munich.

[4] R. K. Long, 1966: Absorption at ruby laser wavelength for low angle total atmospheric paths. Ohio State University, Lab. Tech. Rep. 2156-2, 7.

0021-8952/81/040476-06$05.50

$$U_{on} = K_1 R^{-2}(\beta_R + \beta_M)_{on} \times \exp\left[-2\int_0^R (\sigma_R + \sigma_M + \sigma_A)_{on} dr\right], \quad (2)$$

$$U_{off} = K_2 R^{-2}(\beta_R + \beta_M)_{off} \times \exp\left[-2\int_0^R (\sigma_R + \sigma_M + \sigma_A)_{off} dr\right], \quad (3)$$

where K_1 and K_2 are the systems constants including η, c, J_t, and A from Eq. (1) for the on-line and off-line systems, β_R and β_M stand for the Rayleigh- and Mie-volume backscattering coefficients, σ_R and σ_M are the total volume scattering coefficients produced by Rayleigh and Mie scattering, and σ_A is the absorption coefficient $[=\rho(R)K_\nu(R)]$.

In order to eliminate the Rayleigh and Mie scattering dependencies, the following assumptions were made:

$$\left.\begin{aligned}(\beta_R + \beta_M)_{on} &= (\beta_R + \beta_M)_{off}\\ (\sigma_R + \sigma_M)_{on} &= (\sigma_R + \sigma_M)_{on}\end{aligned}\right\}, \quad (4)$$

which are valid if both wavelengths are close together and if both measurements are made within a few milliseconds (Schotland, 1974). In this case the influence of the turbulence effects on the aerosol structure could be neglected.

By changing the absorption coefficient into $\sigma_{A_{on}} = n\sigma_{on}$, $\sigma_{A_{off}} = n\sigma_{off}$, using n as the number of water vapor molecules, the ratio of the measured voltages is

$$\frac{U_{on}}{U_{off}}(R) = \frac{K_1}{K_2}\exp\left[-2\int_0^R n(\sigma_{off} - \sigma_{on})dr\right] \quad (5)$$

or

$$\ln\left[\frac{U_{off}}{U_{on}}(R)\frac{K_1}{K_2}\right] = 2(\sigma_{off} - \sigma_{on})\int_0^R ndr. \quad (6)$$

In order to eliminate the system constants K_1 and K_2 containing the different energies of both lasers, one uses another value of the ratio [Eq. (5)] at a range $R = R + \Delta R$:

$$\int_0^R ndr = \frac{1}{2(\sigma_{on} - \sigma_{off})}\ln\left[\frac{U_{off}}{U_{on}}(R)\frac{K_1}{K_2}\right], \quad (7)$$

$$\int_0^{R+\Delta R} ndr = \frac{1}{2(\sigma_{on} - \sigma_{off})} \times \ln\left[\frac{U_{off}}{U_{on}}(R + \Delta R)\frac{K_1}{K_2}\right]. \quad (8)$$

Now it is possible to determine the number of water vapor molecules for range intervals between R and $R + \Delta R$ just from the received signals

$$\int_R^{R+\Delta R} ndr = \frac{1}{2(\sigma_{on} - \sigma_{off})} \times \ln\left[\frac{U_{on}(R)}{U_{on}(R + \Delta R)}\frac{U_{off}(R + \Delta R)}{U_{off}(R)}\right]. \quad (9)$$

The light source in our case is a ruby laser which can be tuned over an absorption line. Fig. 1 shows the relative absorption in the ruby laser wavelength region. The spectrum between 0.6942 and 0.6943 μm is used.

3. Lidar system

The ruby lidar DIAL system designed for the determination of vertical profiles of absolute humidity, is shown in Fig. 2. The system consists of two telescopes and two ruby lasers. The larger telescope is used for the humidity measurements. The specifications are listed in Table 1.

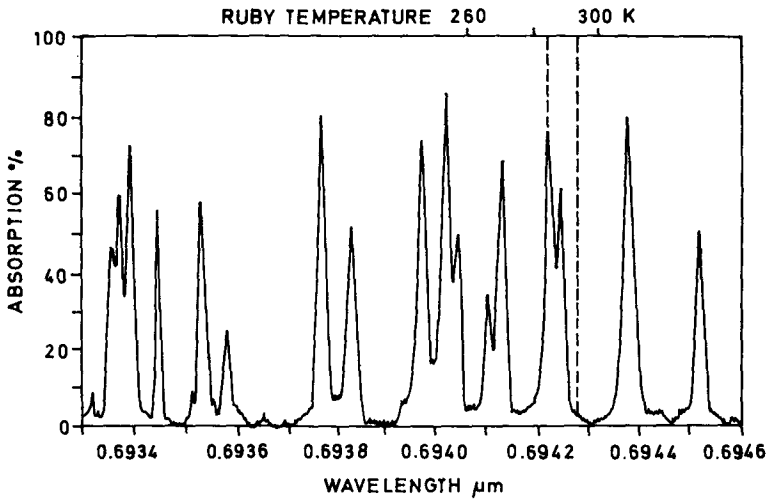

FIG. 1. Atmospheric absorption in the ruby laser wavelength region (after Long, 1966).

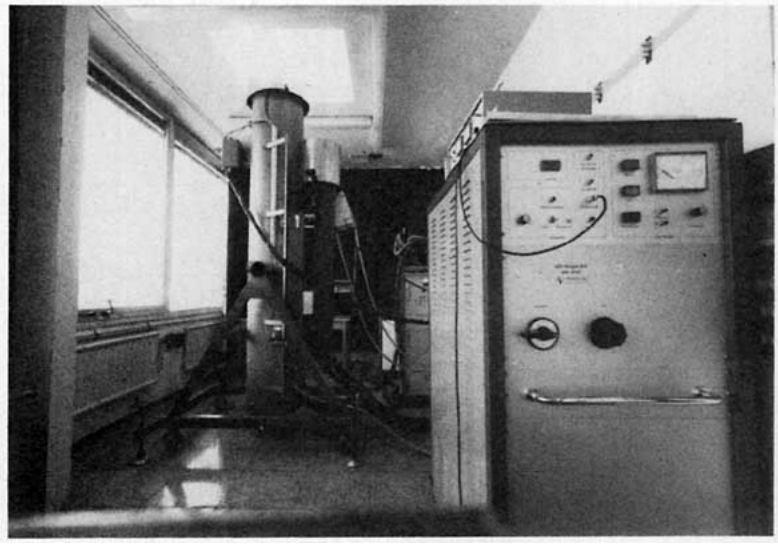

FIG. 2. DFVLR Lidar System IV.

Total overlapping of the laser beams with the telescope field of view occurs at an altitude of ~250 m. The two ruby lasers are temperature controlled and both lasers can be fired within 1 ms. After firing the lasers, it takes up to 3 min for the cooling units to reach the same temperature of the ruby rod again (see pulse repetition rate in Table 1).

For most ruby lidar systems photomultipliers are used to detect the backscattered energy. Photomultipliers are in general more sensitive compared to photodiodes, but there is a need for an interference filter to reduce the sky background radiation, the background noise. For a real lidar, in Eqs. (2) and (3), there is an additional noise signal U_{noise} added. This signal depends on the detector used. For photomultipliers the noise signal is produced by the sky background radiation. Photomultipliers are therefore background limited detectors. For photodiodes the thermal noise prevails, these detectors are thermal noise limited. Eqs. (2) and (3) are now:

$$U_{\text{on}} = U_{\text{signal, on}} + U_{\text{noise, on}}, \tag{2'}$$

$$U_{\text{off}} = U_{\text{signal, off}} + U_{\text{noise, off}}. \tag{3'}$$

For thermal noise limited detectors is $U_{noise,\,on} = U_{\text{noise, off}}$, because there is no interference filter necessary to cut the background noise. If the signal is much greater than the noise ($U_{\text{signal}} \gg U_{\text{noise}}$), Eq. (9) can be used to determine the absolute humidity. This can also be realized for small signals ($U_{\text{signal}} \approx U_{\text{noise}}$) by averaging many signals, because the noise signal will be smaller:

$$U_{\text{noise, } N \text{ times averaged}} = N^{-1/2} U_{\text{noise}}.$$

The backscattered radiation reaches a photodiode (EG&G type YAG 444). Typical performance values for the photodiode are quantum efficiency greater than 50%, responsivity 0.42 A/W, rise time 8–10 ns. For short light pulses the photocurrent is nearly linear up to 1 A. This means that strong echoes from

TABLE 1. Parameters of the DFVLR Lidar System IV.

Transmitter 1		Transmitter 2	
Ruby laser (Impulsphysics)		Ruby laser (Laser Associates Ltd.)	
Wavelength	0.69428 μm	Wavelength	0.6942–0.69428 μm
Line width	<0.00001 μm	Line width	<0.00001 μm
Stability	≈0.00001 μm	Stability	≈0.00001 μm
Output energy	1 J	Output energy	1 J
Pulse duration	20 ns	Pulse duration	20 ns
Pulse repetition rate	5/100 Hz	Pulse repetition rate	5/100 Hz
Receiver 1/Receiver 2	40/25 cm		
Mirror diameter	40/25 cm		
Focal length	250/150 cm		
Photodiode	YAG 444/YAG 444		

clouds cannot damage the diode. The photodiode is operated in the photoconductive mode and can be considered as a current source. The photocurrent is fed into a wideband (100 MHz) differential FET amplifier (Analog Devices type 50K) with an input noise of 6 μV_{rms}. In the feedback circuit 3 resistors can be switched remotely to select a proper amplification. In order to avoid transmission effects for both wavelengths at the diode, no interference filter is used. The small field of view, 8 mrad, reduces the sky background radiation to about 10^{-8} W. The calculated noise equivalent power for the YAG 444 photodiode (detectivity 10^{12} W^{-1} cm $Hz^{1/2}$) combined with a 2 MHz low-pass filter is 1.42×10^{-9} W. The background radiation produces a small low frequency voltage at the amplifier which is blocked by capacitors in the following stages. After the first amplification, the signal is fed into a variable gain amplifier (SG 3402 J). To avoid an overload of the last emitter follower stage, excessive signals, e.g., from clouds, are clipped by diodes.

The energy and wavelength of each laser pulse are measured by a combined energy and wavelength monitor. The energy monitors produce also the trigger signal for the data recording system.

A digital data recording system was added to the lidar. To avoid an electromagnetic interference caused by the laser ignition on the data system, the data system was installed in another room. Two Biomation 8100's are used to store both the on-line and off-line signals, triggered separately by laser 1 and laser 2.

There are two ways for data handling possible, one for an automatic transfer to a computer-compatible tape recorder, the other using two averaging units which are connected to an on-line minicomputer (Commodore PET 2001). From Eq. (9) it results that no additional calibration should be necessary. The same optical path, the same photodiode, and the same amplifiers are used for both signals. Nevertheless, one of the uncertainties is the limited dynamic range of the digitizers. This limited resolution of 8 bits requests similar laser energies for both lasers. The other problem is the accuracy of the linearity of the two Biomations. If one unit deviates from the other unit in the linear transformation of the analog signal into an 8 bit word, an error arises. This possible error was eliminated by a calibration measurement using both lasers at the same temperature or wavelength. There was indeed a small deviation. The quotient Q from the logarithms in Eq. (9)

$$Q = \frac{U_{on}(R)U_{off}(R + 100)}{U_{on}(R + 100)U_{off}(R)}$$

at 20°C for both lasers was estimated by a calibration to 0.963. This value is close to the theoretical expected value 1 and demonstrates the uncertainty of the transient digitizers. Variations of the quotient for equal temperatures from 0.91 to 0.98 were determined. Therefore, the measurement of the absolute humidity was always started with a calibration measurement and was closed with an additional calibration measurement.

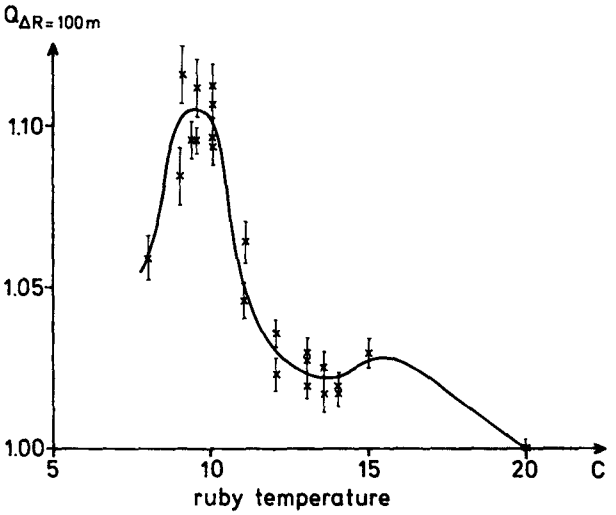

FIG. 3. Measured values of the quotient Q for 100 m range cells versus the ruby temperature.

4. Measurements

a. Determination of the best ruby temperature

For verification of the atmospheric absorption for ruby laser wavelengths shown in Fig. 1 it was necessary to determine the ruby temperature where the maximum absorption by water vapor occurs. Temperatures between 20 and 5°C are easy to handle for an operational system. Laser 2 was tuned from 20°C down to 8°C. Laser 1 was fixed at 20°C. The measurements were made on a horizontal path up to distances of 1200 m.

Fig. 3 shows the results. The quotient Q for 100 m range cells in the atmosphere is plotted versus the ruby temperature. For comparison, the humidity was measured in situ by a wet-bulb and dry-bulb thermometer. The measurements are made at different days during the year and the results shown in Fig. 3 are normalized to 13.33 mb (10 mm Hg) water vapor pressure. The largest absorption cross-section difference was determined from this measurement as

$$\delta_{9.5} - \delta_{20} = 1.43 \times 10^{-27}\ m^2.$$

To get information on accuracy, horizontal measurements from the top of the Institute of Atmospheric Physics of the DFVLR were carried out during 11 months from July 1978 until June 1979. Fig. 4 shows the quotient Q versus the *in situ* measured water vapor pressure. The ruby temperatures were

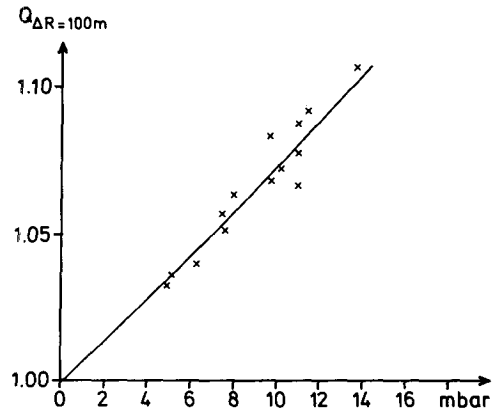

FIG. 4. Measured value of the quotient Q for 100 m range cells versus the *in situ* measured water vapor pressure.

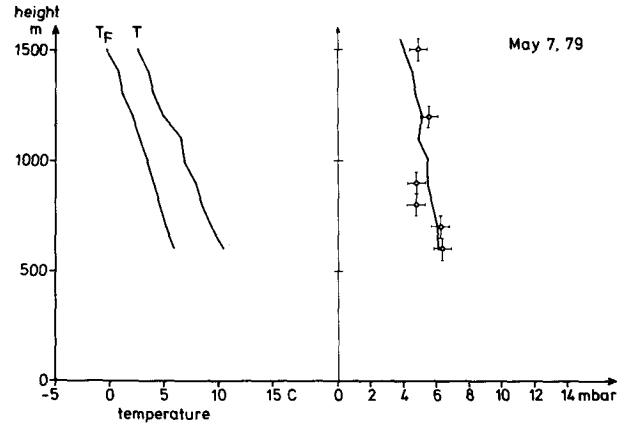

FIG. 6. Comparison of lidar remote and motor glider *in situ* measurements of the absolute humidity on 7 May 1979 (noon).

9.5°C for laser 2 and 20°C for laser 1. The accuracy is in the order of 1 mb water vapor pressure for 100 m range resolution and for mean values of 10 single laser pulse pairs. That means, with the described lidar measurements of the absolute humidity up to distances of 1200 m in range, that resolution of 100 m within 30 min with 1 mb accuracy are possible.

b. Comparisons with radiosonde measurements

The vertical lidar measurements were carried out during daytime. The computer tapes were evaluated at the DFVLR computer center south. Each pulse pair was handled separately. The quotient Q was extracted in range intervals of 100 m starting from 450 m up to 1500 m above ground. Then the results of 20 single measurements were averaged. Fig. 5 shows an example of the comparison of simultaneous balloon and lidar profiles obtained on 16 October 1978. The result of the radiosonde ascent (dew-point and dry-bulb temperature versus height) is shown on the left side of Fig. 5. The comparison of the vertical absolute humidity distribution is drawn on the right side. The solid curve is the radiosonde result, the points are the error bars in altitude (100 m range cells) and in accuracy (1 mb) represent mean values of 20 single lidar measurements. Fig. 5 shows a good general agreement between the two types of measurements.

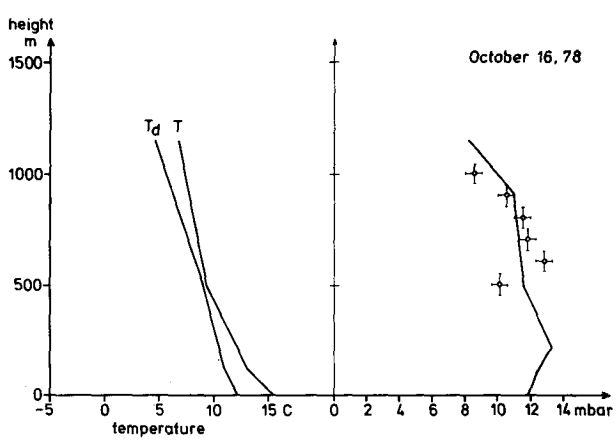

FIG. 5. Comparison of lidar and balloonborne sounding of the absolute humidity on 16 October 1978 (noon).

Another comparison was made during May 1979 with vertical *in situ* measurements using instruments in a motor-assisted glider. This was better for comparison because the radiosonde station is 30 km away from the lidar station. The motor-assisted glider was operated near the institute and made measurements of the dry- and wet-bulb temperature. Flight levels were from 600 m above ground up to 1500 m. Fig. 6 shows the result. The in situ measurement is shown in Fig. 6 left. The comparison with the lidar is on the right side. Compared to Fig. 5, the October measurement, there is less water vapor pressure. There is also a good general agreement in the shape.

The results shown in Figs. 3–6 demonstrate the usefulness of the ruby lidar water vapor absorption measurements for determining of the absolute humidity.

For an operational system there is a need for on-line data processing. By averaging of 10 lidar echoes for both wavelengths in the averager units connected to the transient digitizers Biomation 8100, the absolute humidity distribution can be computed directly. Table 2 shows the results of a measurement taken on 28 June 1979. There was no vertical *in situ* comparison on this day at the same time as the lidar measurement was made; the ground humidity was measured to 13.5 mb. The value is close to the determined humidities.

One step into the direction of an operable system is demonstrated with this on-line data recording, averaging and computing system.

TABLE 2. Results of the vertical absolute humidity distribution measured on-line on 28 June 1979 (1300 GMT).

Height above ground (m)	Ratio U_{off}/U_{on}	Quotient Q (calibration corrected)	Water vapor pressure (mb)	
			Lidar	Radiosonde (1045 GMT)
500	1.137	—	—	9.6
600	1.203	1.095	12.5	9.5
700	1.242	1.069	9.4	9.2
800	1.304	1.087	11.5	8.7
900	1.354	1.075	10.2	8.0

5. Conclusion

Measurements were carried out during 11 months, starting with the determination of the best ruby temperature for making these measurements—over the estimation of the accuracy and comparisons with radiosonde measurements—up to the demonstration of on-line data processing. Some years of preparation were necessary. The results taken under daylight conditions were satisfactory. One step into direction of an operable system is demonstrated.

The operation of such a system consisting of many units is also very difficult for scientists and engineers at research laboratories. For a technician in the weather service it would be too difficult. There is a need for a more operationally oriented system using smaller ruby lasers, such as installed in range finders. With lower power the eye-safety problem can be solved. A faster repetition rate in connection with averager units is then required.

REFERENCES

Blackadar, A. K., and E. G. Droessler, 1977: *Workshop on the Future of National Atmospheric Research*. Boston, Amer. Meteor. Soc.

Cooney, J. A., 1970: Remote measurements of atmospheric water vapor profile using the Raman component of laser backscatter. *J. Appl. Meteor.*, **9**, 182–194.

Dobbins, D. L., and A. H. La Grone, 1969: Number density determination in the atmosphere of O_2, H_2O, and CO_2 gas constituents by use of a high intensity laser beam. *Radio Sci.*, **4**, 407–411.

Hinkley, E. D., 1976: Laser monitoring of the atmosphere. *Topics in Applied Physics*, Vol. 14, Springer-Verlag.

Inaba, H., and T. Kobayasi, 1972: Laser Raman radar. *Optoelectronics*, **4**, 101–123.

Melfi, S. H., 1972: Remote measurements of the atmosphere using Raman scattering. *Appl. Opt.*, **11**, 1605.

Pourny, J. C., D. Renaut and A. Orszag, 1979: Raman lidar humidity sounding of the atmospheric boundary layer. *Appl. Opt.*, **18**, 1141–1148.

Schotland, R. M., 1974: Errors in the lidar measurements of atmospheric gases by differential absorption. *J. Appl. Meteor.*, **13**, 71–77.